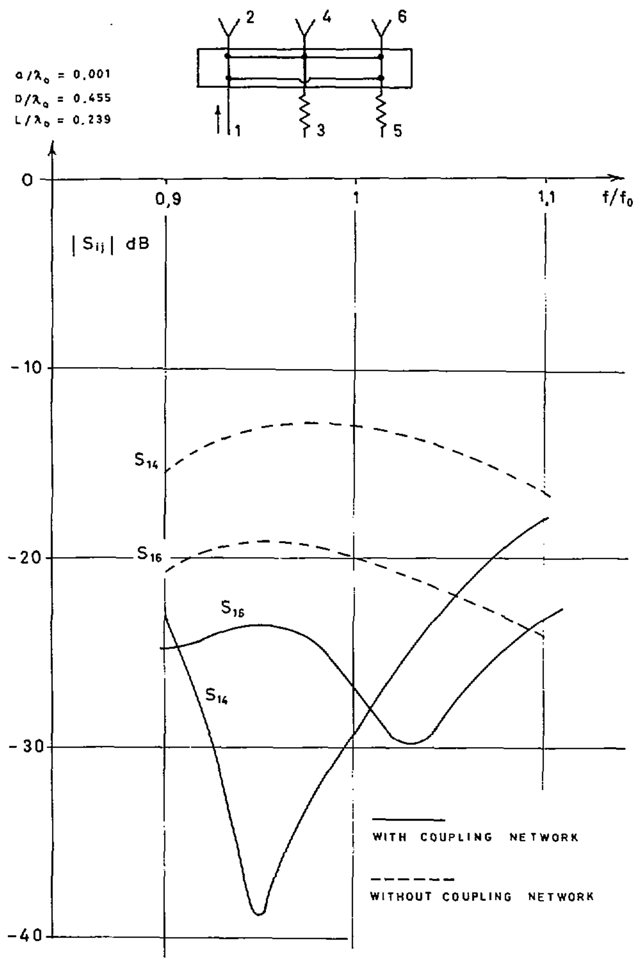

Fig. 8. Numerical results for descattering of three-element linear array of monopoles, with and without network. Network is nonplanar.

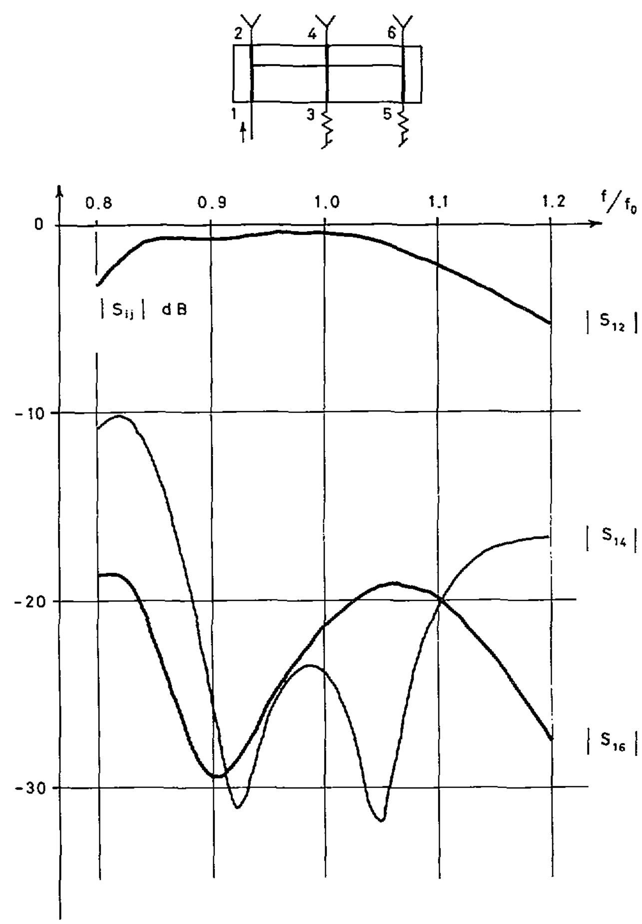

Fig. 9. As in Fig. 8 except that network is planar.

matched, parasitic antenna, but without the network. The pattern in Fig. 7(c) results when the network is included. It is evident that the two antennas are now completely independent. The coupling into the load is very similar to the scattering curves in Fig. 5.

A linear array of three monopoles cannot be descattered completely since a reactive mutual impedance between the two outer elements and adjacent elements cannot be obtained simultaneously. Fig. 8 shows what can be achieved with a nonplanar network and Fig. 9 with a planar network (no direct coupling between the outer lines).

Figs. 8 and 9 are a result of an optimization of the structure, where the deviation of the complete scattering matrix from the ideal scattering matrix at $f = f_0$ is minimized. The scattering coefficients shown are really the antenna currents normalized to the incident current at port 1 under matched conditions.

V. Conclusion

It has been shown theoretically and experimentally that the effects of mutual interaction between two or more antennas may be completely removed by a simple network connecting the lines feeding the antennas. Two conditions must be satisfied: 1) the scattering pattern should equal the transmit pattern for an antenna and 2) the patterns of two antennas should be orthogonal in a multibeam sense, i.e., the mutual impedance should be reactive. The connecting network may consist of transmission lines with a characteristic impedance different from the feeding lines.

References

[1] P. W. Hannan, D. S. Lerner, and G. H. Knittel, "Impedance matching a phased-array antenna over wide scan angles by connecting circuits," *IEEE Trans. Antennas Propagat.*, vol. AP-13, no. 1, pp. 28–34, Jan. 1965.
[2] N. Amitay, "Improvement of planar array match by compensation through contiguous element coupling," *IEEE Trans. Antennas Propagat.*, vol. AP-14, no. 5, pp. 580–586, Sept. 1966.
[3] P. W. Hannan, "Proof that a phased-array antenna can be impedance matched for all scan angles," *Radio Science*, vol. 2 (New Series), no. 3, pp. 361–369, March 1967.
[4] J. L. Allen, "A theoretical limitation on the formation of lossless multiple beams in linear arrays," *IRE Trans. Antennas Propagat.*, vol. AP-9, pp. 350–352, July 1961.
[5] W. D. White, "Pattern limitations in multiple beam antennas," *IRE Trans. Antennas Propagat.*, vol. AP-62, pp. 430–435, July 1962.
[6] W. Wasylkiwskyj and W. K. Kahn, "Theory of mutual coupling among minimum-scattering antennas," *IEEE Trans. Antennas Propagat.*, vol. AP-18, pp. 204–216, March 1970.
[7] J. Bach Andersen, H. A. Lessow, and H. Schjær-Jacobsen, "Coupling between minimum scattering antennas," *IEEE Trans. Antennas Propagat.*, vol. AP-22, no. 6, pp. 832–835, Nov. 1974.

Linearly Polarized Microstrip Antennas

ANDERS G. DERNERYD, STUDENT MEMBER, IEEE

***Abstract*—An equivalent network for square and rectangular shaped microstrip radiating elements is derived. In order to simplify the problem the radiating element is considered as two slots separated by a transmission line of low characteristic impedance. The slots are characterized**

Manuscript received October 28, 1975; revised February 28, 1976.
The author is with the Microwave Antenna Laboratory, Chalmers University of Technology, Gothenburg, Sweden.

by their radiation pattern, directivity, and equivalent admittance. A design procedure for open circuit halfwave resonators and for arrays of such resonators is given. Finally, some antennas in the X band are designed and measured.

Introduction

When conformal and low profile antennas are required, the microstrip antenna is the best choice. This type of antenna also has the advantage of low cost and weight, reproducibility, design flexibility, and ease of installation. The radiating elements together with the feed lines are easily photo-etched on a thin dielectric sheet on a ground plane. The elements may be square, rectangular, round, etc., and they are excited through one or more feed points from the edge or from the back through the ground plane.

The ideas behind the microstrip radiator were published in a communication by Munson [1] where they also were tested on a linear multifeed array. Linearly and circularly polarized antennas from VHF through X band have been built [2]–[8]. The circular polarization has been obtained by two orthogonal excitations in phase quadrature. A single feed point has also been demonstrated to give circular polarization together with a pentagon shaped radiating element [9] or with a feed line at the corner of a rectangular shaped element, [10] and [11]. A drawback of microstrip antennas is the narrow bandwidth, but this can be increased by cutting notches in the radiating sheet [12] or by increasing the ground plane spacing. A dual band microstrip radiating element has also been developed [10].

The purpose of this report is to present an equivalent network and design procedure for square and rectangular shaped microstrip radiators. First, the antenna parameters, such as radiation pattern, directivity, and equivalent admittance, of a single slot are derived. The microstrip radiator is then characterized by two slots separated by a transmission line. The length and the bandwidth of the microstrip resonator are calculated in the next paragraph. Furthermore, a design procedure for linear arrays of microstrip radiators is given. Finally, some experimental antennas are built and evaluated.

Basic Radiator

The microstrip radiating element consists of a conducting sheet spaced a small fraction of a wavelength above a ground plane. A linearly polarized microstrip radiating element is shown in Fig. 1. It consists basically of two slots perpendicular to the feed line and separated by a transmission line of very low impedance. The length of the line is almost half a wavelength to reverse the fields in the slots. The component of the fields parallel to the ground plane adds in phase to give a maximum radiated field normal to the element. The radiation pattern as well as other antenna parameters will now be derived for a single slot antenna.

Radiation Pattern

The electric fields in the slots can be decomposed into a vertical and a horizontal component. The vertical components in the two slots are out of the phase and cancel, while the horizontal components are in phase and add. Let us assume that the horizontal component extends a length equal to the ground plane spacing from the edge of the sheet. The radiated field of the slot can then be calculated from the geometry given in Fig. 2. The electric field is constant in the x direction and zero elsewhere.

$$E = E_x\hat{x}, \qquad |x| \leq \frac{h}{2}. \tag{1}$$

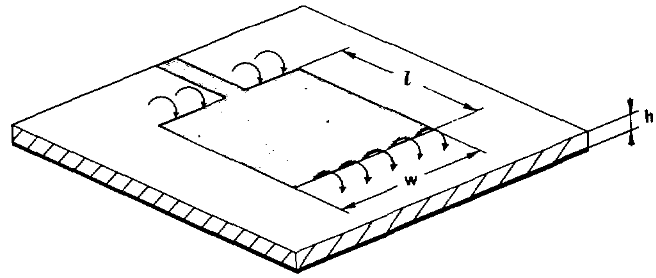

Fig. 1. Linearly polarized microstrip radiating element.

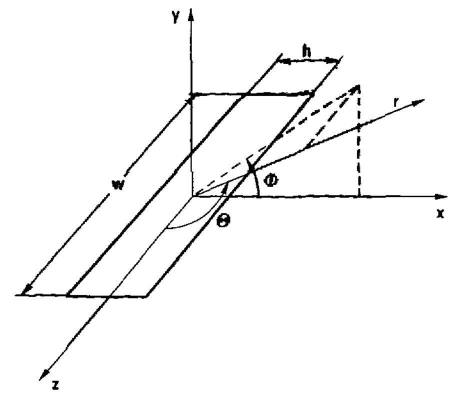

Fig. 2. Geometry of radiating slot.

Higher order modes are neglected, since the number of feedpoints are chosen to excite only the TEM-mode. This slot will produce exactly the same field as a magnetic dipole with the magnetic current

$$I_m = 2E_x\hat{z}, \qquad |z| \leq \frac{w}{2} \tag{2}$$

radiating into free space.

The radiation field at a distance r from the origin may be calculated by a standard method [13]. A potential function generated by the source distribution (2) is found by integrating over the source points.

$$F_z = \frac{e^{-jk_0r}}{4\pi r}\, 2E_xhw\, \frac{\sin\left(\frac{k_0h}{2}\sin\theta\cos\phi\right)}{\frac{k_0h}{2}\sin\theta\cos\phi}\, \frac{\sin\left(\frac{k_0w}{2}\cos\theta\right)}{\frac{k_0w}{2}\cos\theta}. \tag{3}$$

The far-field approximation will only give a ϕ-directed component of the radiated electric field:

$$E_\phi = -jk_0F_z\sin\theta. \tag{4}$$

Defining $V_0 = hE_x$ as the voltage across the slot and considering the height very small, $k_0h \ll 1$, the pattern expression becomes

$$E_\phi = -j\frac{V_0}{\pi}\frac{e^{-jk_0r}}{r}\frac{\sin\left(\frac{\pi w}{\lambda_0}\cos\theta\right)}{\cos\theta}\sin\theta \tag{5}$$

where λ_0 is the free space wavelength.

Radiation Conductance

To determine the total radiated power from the slot we have to integrate the real part of the Poynting vector over a hemisphere of large radius. Since the slot radiates only on one side the

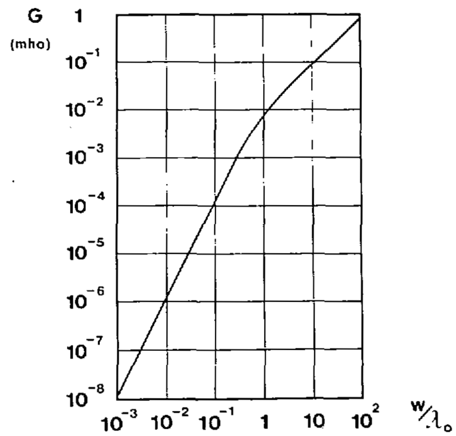

Fig. 3. Slot conductance as function of w/λ_0.

integration is carried out over half the hemisphere. With the field in (5) we get

$$P = \frac{1}{2}\sqrt{\frac{\varepsilon}{\mu}}\frac{V_0^2}{\pi}\int_0^\pi \frac{\sin^2\left(\frac{\pi w}{\lambda_0}\cos\theta\right)}{\cos^2\theta}\sin^3\theta\, d\theta. \tag{6}$$

Since V_0 is the voltage across the center of the slot a radiation conductance may be defined, as the conductance, placed across the center of the slot, which will dissipate the same power as that radiated by the slot:

$$G = \frac{1}{\pi}\sqrt{\frac{\varepsilon}{\mu}}\int_0^\pi \frac{\sin^2\left(\frac{\pi w}{\lambda_0}\cos\theta\right)}{\cos^2\theta}\sin^3\theta\, d\theta = \frac{I}{120\pi^2}. \tag{7}$$

The integral I can be solved by numerical methods and a plot of the radiation conductance as a function of w/λ_0 is shown in Fig. 3. For small values of the width, $w/\lambda_0 \ll 1$, the integration can be approximated to give

$$G = \frac{1}{90}\left(\frac{w}{\lambda_0}\right)^2. \tag{8}$$

When w tends to infinity the conductance is

$$G = \frac{1}{120}\frac{w}{\lambda_0} \tag{9}$$

in accordance with [1].

Slot Capacitance

An equivalent susceptance at the slot, represented by a capacitor, due to the end effect is given by Hammerstad [14]. He gives an approximate expression for the normalized line extension Δl of an open microstrip circuit:

$$\frac{\Delta l}{h} = 0.412\frac{\varepsilon_e + 0.300}{\varepsilon_e - 0.258}\frac{w/h + 0.262}{w/h + 0.813} \tag{10}$$

where ε_e is the effective dielectric constant. Curves of the normalized line extension as a function of w/h are shown in Fig. 4 with the effective dielectric constant as a parameter. An equivalent end capacitance can now be found:

$$C = \frac{\Delta l}{vZ_0} \tag{11}$$

where Z_0 is the characteristic impedance and v is the phase velocity.

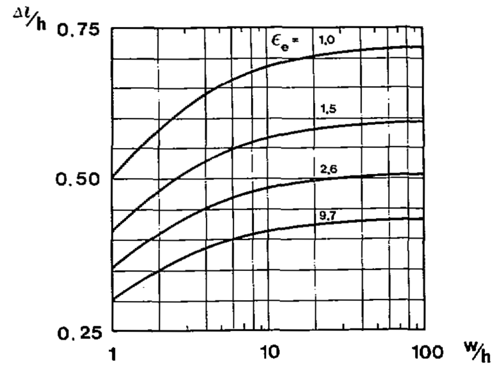

Fig. 4. Normalized line extension of open microstrip circuit as function of w/h and ε_e.

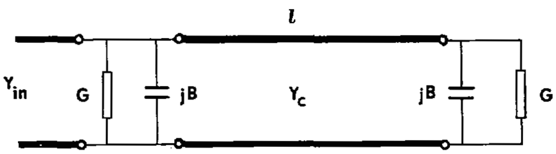

Fig. 5. Equivalent network of microstrip radiating element.

Directivity

Another quantity of interest in the description of antenna performance is the directivity. This quantity is defined as the ratio between the maximum power density and the average radiated power density at a certain range. The directivity of the slot can be calculated to give

$$D = \frac{4\pi^2 w^2}{I\lambda_0^2}. \tag{12}$$

For small slots, $w/\lambda_0 \ll 1$, the directivity approaches 3, which is equivalent to 4.8 dB as expected for a short slot radiating into half space.

Halfwave Resonator

The halfwave microstrip resonator can now be represented by an equivalent network. This model will be treated with network techniques to calculate input admittance and bandwidth.

Equivalent Network

The halfwave resonator in Fig. 1 radiates from the open ends while the radiation from the strip is negligible for wide strips (characteristic impedance > 50 ohm). The microstrip radiating element can therefore be represented by two slots separated by a transmission line of low characteristic impedance as shown in Fig. 5. The input admittance of a radiating element can be found by transforming one of the slots through the low impedance line to give

$$Y_{\text{in}} = G + jB + Y_c\frac{G + j(B + Y_c\tan\beta l)}{Y_c - B\tan\beta l + jG\tan\beta l} \tag{13}$$

where β is the propagation constant and l is the length of the transmission line.

The radiating element is resonant, when the imaginary part of the input admittance cancels. This occurs when the length of the line is

$$\tan\beta l = \frac{2Y_cB}{G^2 + B^2 - Y_c^2}. \tag{14}$$

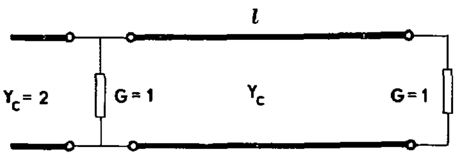

Fig. 6. Equivalent network for bandwidth calculations.

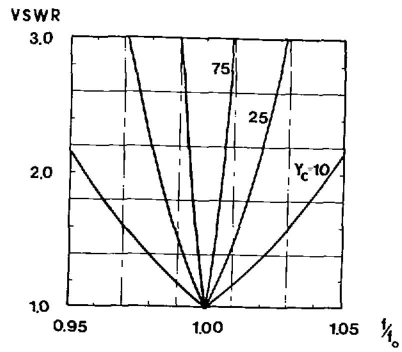

Fig. 7. VSWR as function of f/f_0.

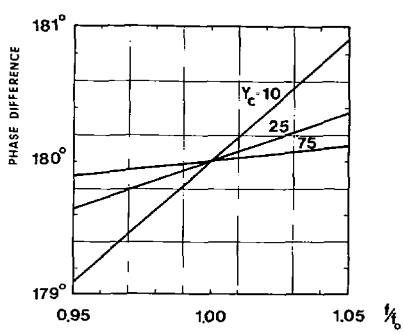

Fig. 8. Phase difference as function of f/f_0.

Practical values of the parameters give a resonant length slightly shorter than half a wavelength. The input admittance at resonance is

$$Y_{\text{in}} = 2G. \tag{15}$$

Bandwidth

Consider the network in Fig. 6. When the electric length of the transmission line is half a wavelength, the input line is matched. Curves of the VSWR on the input line are shown in Fig. 7 as a function of the relative frequency. The higher the characteristic admittance of the transmission line is, the narrower is the bandwidth, typically a few percent. The phase difference between the voltages across the loads are shown in Fig. 8. As can be seen, the change in phase is not critical for the radiation pattern, when the length of the transmission line is changed.

Linear Arrays

When greater directivity is required than can be obtained by a single element, antenna arrays are used. Microstrip halfwave resonators can be cascaded to form a linear array. The dimensions of the array will be calculated from the network model to give maximum gain.

Equivalent Network

Microstrip radiating elements can be fed in series to form a linear array. The connecting transmission lines ought to be

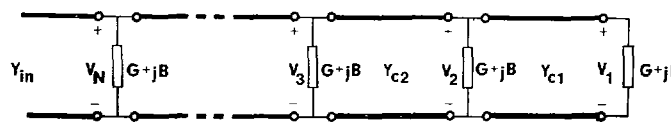

Fig. 9. Equivalent network of linear microstrip array.

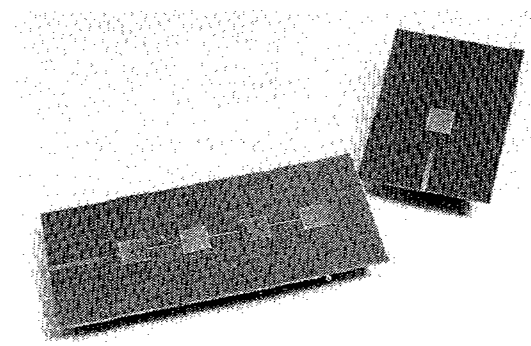

Fig. 10. Microstrip antennas for X band.

chosen narrow in order not to disturb the fields in the slots. An equivalent network of $N/2$ cascaded radiating elements can now be obtained, since the basic slot is fully characterized. The network model is shown in Fig. 9. From this model the array factor is immediately calculated

$$\text{AF} = \sum_{n=1}^{N} V_n \, e^{jk_0 d_n \cos\phi} \tag{16}$$

where d_n is the distance between the first and the nth slot and k_0 is the propagation constant in free space.

Optimization

In order to maximize the gain of the array the dimensions of the radiating elements as well as the connecting transmission lines had to be found. The function to be maximized is the ratio between the radiated and the input power. To get the main beam normal to the array the function to be optimized is

$$G_{\text{AF}} = \frac{\left|\sum_{n=1}^{N} V_n\right|^2 G}{|V_N|^2 R_e\{Y_{\text{in}}\}}. \tag{17}$$

The parameters to be changed are the length of the microstrip radiators and the distances between them. The array factor will give an addition in directivity equal to

$$D_{\text{AF}} = \frac{\left|\sum_{n=1}^{N} V_n\right|^2}{\sum_{n=1}^{N} |V_n|^2}. \tag{18}$$

Experimental Arrays

To verify the theory some X band microstrip array antennas of different sizes were built and tested. First a single element was made and later on arrays with different numbers of elements. Two of these microstrip antennas are shown in Fig. 10.

Single-element Antenna

A square microstrip radiating element was designed at 9 GHz. The equivalent admittance of the basic slot is found to 0.000922 +

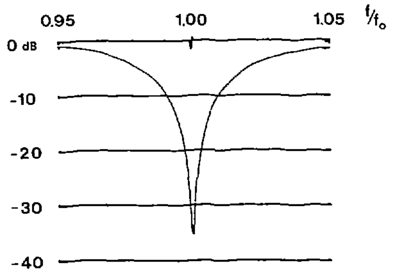

Fig. 11. Reflection coefficient of single microstrip antenna as function of f/f_0.

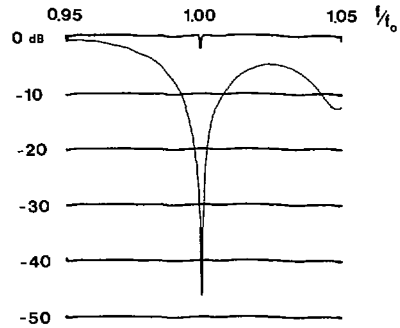

Fig. 12. Reflection coefficient of four-element microstrip array as function of f/f_0.

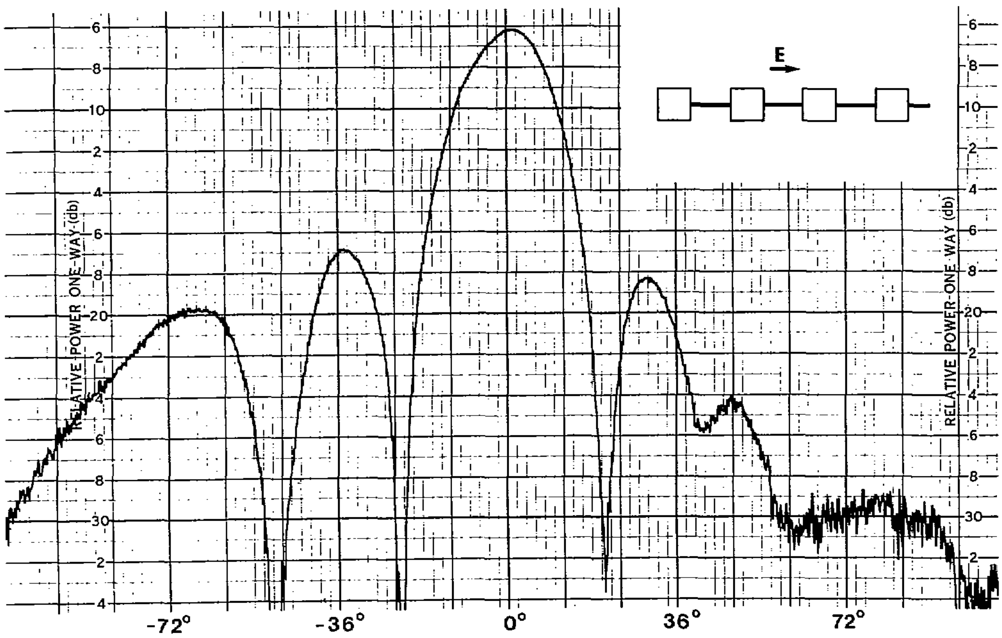

Fig. 13. E-plane radiation pattern of four-element microstrip array.

$j0.00745$ mhos by using (7), (10), and (11). The length of the element to give a real input admittance is given by (14) to 0.46λ with a characteristic impedance of 15 ohm. The directivity of the element is almost twice that of a single slot and is given by (12) to 6.3 or 8.0 dB. According to Fig. 8 the bandwidth is 1.5 percent with $Y_c = 72$ and for a VSWR < 2. The antenna was matched to 50 ohm by a quarterwave transformer and the reflection coefficient was measured. The result is shown in Fig. 11. The bandwidth is 2 percent for a VSWR less than two and the gain was measured to 7.6 dB with a loss in the feed line of 0.3 dB.

Four-element Array

The single element was then used in a four-element linear array at 9 GHz. The feed line between the elements was a transmission line of high characteristic impedance (100 ohm) so as not to disturb the field in the slots too much. The length of the radiators and the distance between them were varied by means of a computer in order to maximize (17). The increase in gain due to the array factor was calculated to 8.7 dB with a dissipation factor of 0.0008 for the used laminate. The gain of the slot is about 5 dB which gives a total gain of 13.7 dB. The array was then built and tested. The reflection coefficient was measured and is shown in Fig. 12. The bandwidth is 1.7 percent for a VSWR less than two. The gain of the array was measured to 13.3 dB with a loss in the feed line of 0.3 dB. The radiation patterns were also recorded. The E- and H-plane patterns are shown in Figs. 13 and 14, respectively. The sidelobe level is 11 dB and the beamwidth is 20° in the E-plane and 68° in the H-plane.

Conclusions

The principles of the open circuit microstrip radiating element have been investigated. The element has been simplified to two slots separated by a transmission line. The slot has been characterized by its radiation pattern, directivity, and equivalent admittance. The resonant length of the microstrip radiator as well as the optimum dimensions of a linear array have also been derived. Finally, the theory has been demonstrated on some microstrip antennas in the X band. The theory presented here can easily be applied to two-dimensional arrays for linear or circular polarization.

Acknowledgment

The author wishes to thank Prof. E. F. Bolinder, Head of the Division of Network Theory, Chalmers University of Technology, for his support during this work. The investigation was initiated by AB Almex, Stockholm, Sweden.

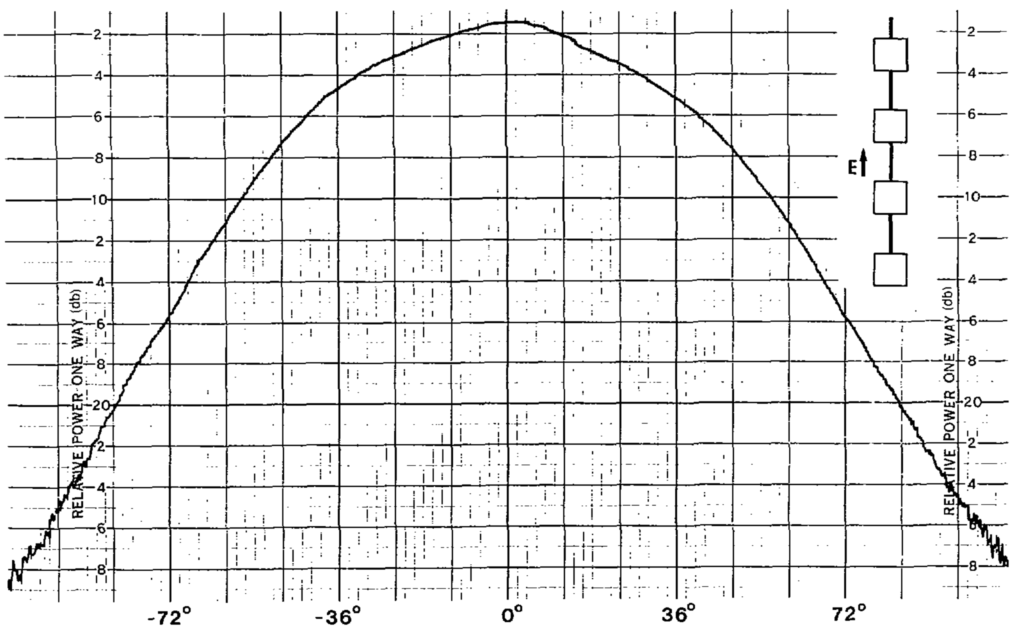

Fig. 14. *H*-plane radiation pattern of four-element microstrip array.

References

[1] R. E. Munson, "Conformal microstrip antennas and microstrip phased arrays," *IEEE Trans. Antennas Propagat.* (Commun.), vol. AP-22, pp. 74–78, Jan. 1974.

[2] J. Q. Howell, "Microstrip antennas," *IEEE Group on Antennas and Propagation Int. Symp.*, p. 177, Dec. 1972.

[3] G. G. Sanford, "Conformal microstrip phased array for aircraft tests with ATS-6," *National Electronics Conf.*, vol. 29, pp. 252–257, Oct. 1974.

[4] J. Q. Howell, "Microstrip antennas," *IEEE Trans. Antennas Propagat.*, vol. AP-23, pp. 90–93, Jan. 1975.

[5] C. W. Garvin *et al.*, "Low profile, electrically small missile base mounted microstrip antennas," *IEEE Society on Antennas and Propagation Int. Symp.*, pp. 244–247, June 1975.

[6] G. Sanford and L. Klein, "Development and test of a conformal microstrip airborne phased array for use with the ATS-6 satellite," *IEE Int. Conf. on Antennas for Aircraft and Spacecraft*, pp. 115–122, June 1975.

[7] J. R. James and G. J. Wilson, "New design techniques for microstrip antenna arrays," *5th European Microwave Conf.*, pp. 102–106, Sept. 1975.

[8] F. R. Zboril, "New antennas on new nonmetallic materials," *5th European Microwave Conf.*, pp. 658–662, Sept. 1975.

[9] H. D. Weinschel, "A cylindrical array of circularly polarized microstrip antenna," *IEEE Society on Antennas and Propagation Int. Symp.*, pp. 177–180, June 1975.

[10] G. G. Sanford and R. E. Munson, "Conformal VHF antenna for the Apollo–Soyuz test project," *IEE Int. Conf. on Antennas for Aircraft and Spacecraft*, pp. 130–135, June 1975.

[11] L. T. Ostwald and C. W. Garvin, "Microstrip command and telemetry antennas for communications technology satellite," *IEE Int. Conf. on Antennas for Aircraft and Spacecraft*, pp. 217–222, June 1975.

[12] W. Wiesbeck, "Miniaturisierte Antenne in Mikrowellenstreifenleitungstechnik," *Nachrichtentechn. Zeitschrift*, vol. NTZ-28, pp. 156–159, May 1975.

[13] W. L. Weeks, *Antenna Engineering.* New York: McGraw-Hill, 1968, pp. 8–26.

[14] E. O. Hammerstad, "Equations for microstrip circuit design," *5th European Microwave Conf.*, pp. 268–272, Sept. 1975.

Radiation from Aperture-Fed Paraboloids Employing Source-Multipole Expansions

M. S. NARASIMHAN, MEMBER, IEEE, AND
K. S. BALASUBRAMANYA, STUDENT MEMBER, IEEE

***Abstract*—A multipole expansion technique to study radiation from aperture antennas in the form of an open-ended waveguide-horn is presented. Particular attention is paid to dual-mode and corrugated circular horns. The radiation pattern of these feeds, derived in terms of multipole moments, is in the form of an algebraic series which converges very rapidly. Further, based on the multipole-expansion technique presented, the far-zone fields of an axially-symmetric aperture-fed paraboloid are obtained in closed form. It is demonstrated that there is a drastic reduction in computer time by using this technique instead of the conventional numerical integration procedure for calculating the far-zone fields of the paraboloid.**

Manuscript received August 17, 1975; revised February 2, 1976. This work was supported in part by the Council of Scientific and Industrial Research.

The authors are with the Department of Electrical Engineering, Indian Institute of Technology, Madras, Madras-600036, India.

Nomenclature

x,y,z	Rectangular coordinates of a field point.
$\bar{a}_x,\bar{a}_y,\bar{a}_z$	Unit vectors associated with (x,y,z).
r,θ,ϕ	Spherical coordinates of a field point.
$\bar{a}_r,\bar{a}_\theta,\bar{a}_\phi$	Unit vectors associated with (r,θ,ϕ).
$\bar{n}$	Unit vector normal to the surface under consideration.
E_r,E_θ,E_ϕ	Components of the electric field intensity.
H_r,H_θ,H_ϕ	Components of the magnetic field intensity.
$\bar{J}_e$	Electric surface current density.
$\bar{J}_m$	Magnetic surface current density.
$\bar{A}_e(\bar{r})$	Electric vector potential.
$\bar{A}_m(\bar{r})$	Magnetic vector potential.
$J_n(x)$	Bessel function of first kind, order n.
$J_n'(x)$	First derivative with respect to the argument of $J_n(x)$.
λ	Free space wave length.
k	$2\pi/\lambda$.
ω	Angular frequency.
μ	Permeability of free space.
ε	Permitivity of free space.
Z_0	Intrinsic impedance of free space.
a	Aperture radius of the horn.
θ_0	Half angle subtended by the parabola at the focus.
F	Focal length of the paraboloidal reflector.
A,A_1	Electric field amplitude coefficients.

I. Introduction

In a recent paper Rusch has presented a multipole-expansion technique for calculating the far-fields of an axially symmetric paraboloid fed by a linear current feed [1]. This technique enables one to replace the two-dimensional scattering integral associated with the paraboloid by a rapidly converging algebraic